Salt Permeation and Exclusion in Hydroxylated and Functionalized Silica Pores

Kevin Leung,* Susan B. Rempe, and Christian D. Lorenz
Sandia National Laboratories, MS 1415, 0310, & 1110, Albuquerque, New Mexico 87185, USA
(Received 30 August 2005; published 9 March 2006)

We use combined *ab initio* molecular dynamics (AIMD), grand canonical Monte Carlo, and molecular dynamics techniques to study the effect of pore surface chemistry and confinement on the permeation of salt into silica nanopore arrays filled with water. AIMD shows that 11.6 Å diameter hydroxylated silica pores are relatively stable in water, whereas amine groups on functionalized pore surfaces abstract silanol protons, turning into NH_3^+. Free energy calculations using an *ab initio* parametrized force field show that the hydroxylated pores strongly attract Na^+ and repel Cl^- ions. Pores lined with NH_3^+ have the reverse surface charge polarity. Finally, studies of ions in carbon nanotubes suggest that hydration of Cl^- is more strongly frustrated by pure confinement effects than Na^+.

DOI: 10.1103/PhysRevLett.96.095504 PACS numbers: 61.46.−w, 68.08.De, 68.43.Bc, 66.10.−x

The permeation and exclusion of salt in nanoconfined aqueous media is central to both selective ion transport and purification or desalination of sea and brackish water. The recent synthesis of highly ordered, nanoporous, functionalized silica thin films [1,2], transport experiments in slitlike nanofluidic channels [3,4], and theoretical study of single wall carbon nanotube (SWNT) membranes [5] underscore the timeliness of using water-filled nanoporous materials to study the effect of pore surface chemistry and confinement on salt hydration.

Confinement has long been known to reduce the hydration free energy or Born self energy (ΔG_{hyd}) of electrolytes in aqueous channels [6,7]. A recent quasichemical theory [8] shows that the inner and outer hydration shell contributions to ΔG_{hyd} in bulk water are comparable. This suggests that nanopores with diameter less than 12 Å can potentially frustrate the outer shell hydration (by ~10 kcal/mol), effectively excluding salts from the pores. Currently nanoporous silica membranes have pore diameters down to 2 nm [1]; functionalizing the pore interior and/or applying atomic layer deposition have the potential to achieve subnanometer pores [2]. In such solid state pores, surface chemistry and charge distributions will also be critically important in controlling ion permeation. While ion transport in thin trans-cell membrane biological channel settings (~20 Å in length) has been the subject of extensive theoretical studies [7,9–11], porous silica materials have submicron thickness [1,2]. SWNT's, proposed as a new, salt-excluding, reverse osmosis membrane material [5], also have large aspect ratios. In this work, we model these systems as infinitely long pore arrays, and focus on the material aspects, and on computing the potential of mean force (PMF) inside the water-filled channels.

First we consider the surface chemistry of model amorphous silica pores (Fig. 1). We focus on *p*H at zero charge conditions throughout this work; thus the silica framework is overall charge neutral. While atomistic modeling of water and electrolyte inside wide silica pores have been performed [12], molecular force fields that accurately capture all aspects of silica-water-ion interactions, polarizability or dielectric properties, and deprotonation of surface silanol (−SiOH) groups [13] do not yet exist. Therefore, we design a model system that permits a combined quantum and molecular dynamics (MD) treatment. Figure 1 depicts the $L_x \times L_y \times L_z = 17.1 \times 17.4 \times 15.3$ Å^3 unit cell of this pore array, periodically replicated in all directions. (1) We first generate an amorphous silica solid of appropriate mass density [14]. (2) Next, $a \sim 11.6$ Å diameter cylindrical void is created, and all undercoordinated Si atoms are terminated with −OH. The unit cell contains 70 Si, 158 O, and 38 H atoms. This diameter would imply 6.8 silanol groups per nm^2 if the pore is featureless. However, the pore surface is corrugated and $a \sim 3$ Å diameter passage exists between adjacent unit cells; thus actual silanol density should be closer to the experimental value (5/nm^2) [15]. (3) The pore geometry is optimized using the VASP density functional theory (DFT) code [16] with the PW91 exchange correlation functional [17]. (4) Freezing all silica atoms except the surface silanol protons, we use the grand canonical Monte Carlo (GCMC) technique to determine the water content [18]. We apply the SPC/E water model [19] and silica force fields with partial charges fitted to the *ab initio* electrostatic potential of a $Si_{14}O_{21}H_{30}$ cluster [20], and 12/6 Lennard-Jones (LJ) terms fitted to DFT/PW91 calculations of water adsorption on crystalline silica surfaces [21]. On average, 41 H_2O molecules reside in the unit cell.

Strained silica rings are known to react with H_2O to form silanol groups with low energy barriers [22], in picosecond time scales at $T = 300$ K [23]. To examine the stability of our model hydroxylated pore in water, we conduct *unconstrained ab initio* molecular dynamics (AIMD) at an elevated temperature of 375 K using the DFT code/method mentioned above. A 0.5 fs time step and molecular mechanics preequilibrated starting configurations are used. No chemical reaction or H_2O incorporation into the silica framework occurs within ~4.5 ps, showing that our model pore array is relatively stable at this *p*H.

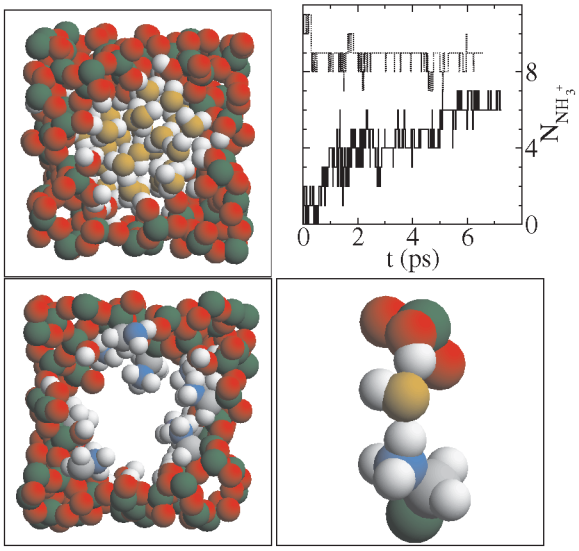

FIG. 1 (color). Counterclockwise from upper left: water-filled silica pore unit cell; silica pore functionalized with $-CH_2NH_3^+$ (water removed for clarity); expanded view of a $-CH_2NH_2$ group in the process of abstracting a proton from H_2O; total number of $-NH_3^+$ groups as a function of time in two AIMD trajectories, starting with 0 and 11 $-NH_3^+$, respectively. The first three panels are AIMD snapshots, and periodic boundary conditions apply in all three directions. Green spheres: Si; red/yellow: O; blue: N; white: H; gray: C.

Functionalized pores behave qualitatively differently. Experimentally, a fraction of the pore surface -OH groups have been successfully replaced with $-(CH_2)_3NH_2$ groups [2]. Thus, in a second model, we randomly replace 11 of the 38 surface $-$SiOH in our unit cell with $-SiCH_2NH_2$. Because silanol groups are acidic and amines are basic, proton transfer may occur. However, NH_3^+ is usually stabilized with hydrogen bonding to 3 H_2O molecules [24], and there are only 35 H_2O in the pore. To determine the NH_3^+ content, we apply AIMD. We examine two initial conditions—one with all $-NH_2$ terminations, the other with all $-NH_3^+$, with the 11 $-$SiOH closest to the ammonium groups deprotonated to preserve charge neutrality (Fig. 1). We graft a CHARMM22 [25] and DFT/PW91-fitted description of the amine/ammonium groups to our silica force fields, and use them to preequilibrate the initial configurations.

Figure 1 depicts the evolution of the number of $-NH_3^+$ ($N_{NH_3^+}$). The AIMD trajectory starting with all $-NH_3^+$ rapidly equilibrates to $N_{NH_3^+} \sim 8.8$. In the one starting with $N_{NH_3^+} = 0$, although equilibration of the titratable protons has not been achieved in 7 ps, most $-NH_2$ have turned into $-NH_3^+$, either by abstracting a proton directly from a nearby SiOH or by indirect transfer via a bridging H_2O (Fig. 1). The fast proton hopping rate is reminiscent of that between adjoining $-NH_2$/-COOH groups in glycine [24]. Thus, AIMD shows that a majority of the amine groups exist in water-filled pores as $-NH_3^+$, stabilized by hydrogen bonds to framework silica oxygens as well as water. Hereafter we assume they are all $-NH_3^+$. NH_3^+ protrude into the pore center while the compensating SiO^- reside closer to the pore surface. As will be shown, this yields a charge distribution, and a PMF [$W(x, y, z)$] for ions, dramatically different from hydroxylated pores.

Next, we use the aforementioned silica force fields to sample $W(x, y, z)$ for Cl^- and Na^+. (AIMD is too costly for this purpose.) We use LJ-based ion force fields [26], with σ_{Na^+} adjusted to 2.4 Å, so that in bulk water Cl^- and Na^+ exhibits ΔG_{hyd} of -90.9 and -88.8 kcal/mol, respectively. We apply umbrella sampling to obtain $\bar{W}(z)$, the PMF averaged over x, y, by adding a harmonic bias along z but otherwise allowing the ions to move freely. $\bar{W}(z)$ is shifted to match thermodynamic integration (TI) results for $W(x, y, z)$ along the pore axis, $x = L_x/2$, $y = L_y/2$, in sampling windows where the pore center is found to be most favored. Electrostatic contributions to TI are computed by applying a 2-point integration formula to the ionic charge [27]. The packing contribution to TI from inserting uncharged LJ spheres in water is about 1 kcal/mol, and further should largely cancel between bulk and confined water; thus it will be neglected. 15–90 ns and 0.2–1 ns MD trajectories are used for each umbrella sampling window/TI calculation.

Figure 2(a) highlights the dramatic effect of confining ions inside narrow, water-filled, hydroxylated pores. Cl^- (Na^+) is strongly destabilized (stabilized). The large, almost equal but opposite effect on Cl^-/Na^+ suggests that the repulsion/attraction is due to electrostatic interactions with the polar pore surface [28]. Figure 2(c) shows that functionalization with 11 NH_3^+ groups (and compensating SiO^-) indeed reverses this polarity, except for a Na^+ trap site.

The PMF depicted in Fig. 2 is computed by placing one ion in the unit cell (Fig. 1). Our objective is the dilute limit, i.e., for a single ion in an $n \rightarrow \infty$ pore array, with a simulation cell ("supercell") made up of n^3 unit cells replicated n times periodically in all directions. Table I shows that $W(L_x/2, L_y/2, z)$ for $n = 1$ is already converged to 2 kcal/mol—but only after we have added the Ewald self-energy, which is large (-27.3 kcal/mol) for $n = 1$ and is appropriate because the water present in the pore array effectively screens the ion-ion image interaction. Extrapolating to $n = 3$, the axis of the hydroxylated pore repels (attracts) Cl^- (Na^+) by an average of $+25.8$ (-22.0) kcal/mol relative to bulk liquid water.

These results are slightly force field dependent. Applying TI to the partial charges and LJ parameters of another silica force field [12] yields $W(L_x/2, L_y/2, z)$ for Cl^-/Na^+ that differ by $\sim \pm 4$ kcal/mol. The results also depend on pore surface structure and silanol coverage.

In hydroxylated pores, the variations in $\bar{W}(z)$ and in $W(L_x/2, L_y/2, z)$ computed via TI at 10 equally spaced positions along the pore axis agree to within 2 kcal/mol [Fig. 2(a)], indicating that the latter is a good measure of

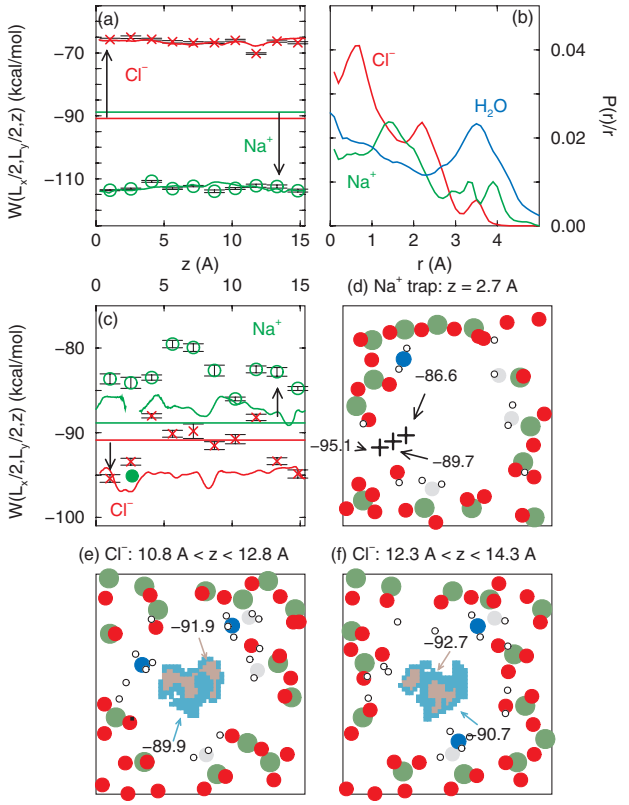

FIG. 2 (color). (a), (b) refer to hydroxylated pore arrays, (c)–(f) to $-CH_2NH_3^+$ lined systems. (a), (c) Crosses/open circles: potential of mean force for Cl^-/Na^+ frozen along the pore axis. Solid curves: umbrella sampling $\bar{W}(z)$ for *unconstrained* Cl^- (red) and Na^+ (green). Horizontal lines: ΔG_{hyd} for Cl^-/Na^+ in bulk water. Panel (c), filled circle: Na^+ trap site at the pore surface. (b) Radial distribution of Cl^- (red), Na^+ (green), and H_2O (blue) in hydroxylated pores. (d) Na^+ at and near trap site (pluses) at $z = 2.7$ Å; (e), (f) Regions where Cl^- free energy is at or below the listed values are shown in color. Atom key: see Fig. 1; water removed for clarity.

ion permeability in such pores. This is consistent with the fact that the radial density of ions divided by r (the distance from the pore axis, and volume element in polar coordinates), $P(r)/r$, is relatively r independent, and there are no trap sites. The H_2O oxygen $P(r)/r$ in hydroxylated pores [Fig. 2(b)] trails off at $r = 4.25$ Å yielding our estimate of an 11.6 Å pore diameter after accounting for the size of H_2O. The two peaks in $P(r)/r$ suggest that this pore can accommodate one water molecule at the center and a water shell around it. Overall, Cl^- is found to prefer the pore center [Fig. 2(b)]. Its $P(r)/r$ also exhibits features at the "trough" of the H_2O radial distribution. Na^+ has a higher concentration at the $-OH$ line pore surface.

TABLE I. $W(L_x/2, L_y/2, 13.3\ \text{Å})$/kcal/mol in hydroxylated pore supercells, computed via thermodynamic integration.

Ion/cell	$n = 1$	$n = 2$	$n = 3$
Cl^-	-66.3 ± 0.3	-62.9 ± 0.7	-64.5 ± 0.8
Na^+	-112.3 ± 0.5	-111.5 ± 0.6	-110.1 ± 0.8

In the NH_3^+ lined model silica pores, $W(L_x/2, L_y/2, z)$ is less useful. The free energy contours in Figs. 2(e) and 2(f) show that Cl^- exhibits more tendency to sample the pore surface near NH_3^+ groups. Hence, in some umbrella windows, a radial $0.5r^2$ kcal/mol/Å^2 potential is applied, and its effect is removed by reweighting, to facilitate sampling. Na^+ can also reside off center to avoid protruding NH_3^+ (not shown). With the pore interior now generally unfavorable, Na^+ is found to be strongly trapped at the aforementioned passageway in the pore wall, which is devoid of NH_3^+ groups [Figs. 2(c) and 2(d)]. One-dimensional umbrella sampling does not readily converge near this Na^+ trap, but TI reveals that it is deep and localized [Fig. 2(d)]. $W(x, y, z)$ rapidly relaxes to pore centerlike values as r decreases, yielding a large free energy barrier against escape. Thus, this trap should always be occupied by an immobile Na^+, which does not readily take part in ion *transport* but should be considered part of the functionalized silica framework. It will repel other Na^+, making the pore even more unfavorable towards Na^+. Thus we expect that the pore polarity reversal of silica pores suggested by the Na^+ $\bar{W}(z)$ [Fig. 2(c)] is qualitatively unchanged by this rare, deep trap. Indeed, polarity reversal via $-NH_3^+$ functionalization has recently been demonstrated in 40 nm wide nanofluidic channels [4]. Figure 2(c) demonstrates this general behavior, but also points out that incomplete NH_3^+ coverage may lead to isolated cases of Na^+ trapping.

The results discussed so far convolve confinement and pore surface polarity effects. To isolate the pure confinement contribution [6], we also consider water-filled (18, 18) SWNT placed in a 18×18 Å^2 square lattice. This nanotube has an 11.4 Å pore diameter, similar to our silica pore, but carries no charges. We apply force fields that reproduce the experimental graphite-water contact angle [29]. GCMC calculations show that this SWNT exhibits a water density similar to that in our silica pores: 46 H_2O molecules per 17.04 Å tube length.

Figure 3(a) shows that $n = 1$ supercells converge TI-predicted $W(L_x/2, L_y/2, z)$ to within 2.5 kcal/mol, similar to silica pores [28]. SWNT pores of this size thus show little confinement penalty for Na^+, in agreement with Ref. [30], but Cl^- is surprisingly unfavorable by 12.6 kcal/mol relative to bulk water. This "pure" confinement effect is smaller than, and nonadditive to, the electrostatic contribution in hydroxylated silica pores. The $P(r)/r$ depicted in Fig. 3(b) shows that layering is more pronounced for H_2O in SWNT than in silica pores, where there is substantial surface inhomogeneity. Na^+ is lodged between two shells of water, while Cl^- prefers the pore center [31]. Preferential transport of Na^+ over Cl^- has been reported for model transmembrane channels [31,32]; the asymmetry between Cl^- and Na^+ likely arises from outer water shell contributions, and is related to ion size, charge, and the hydrogen bond network of first hydration

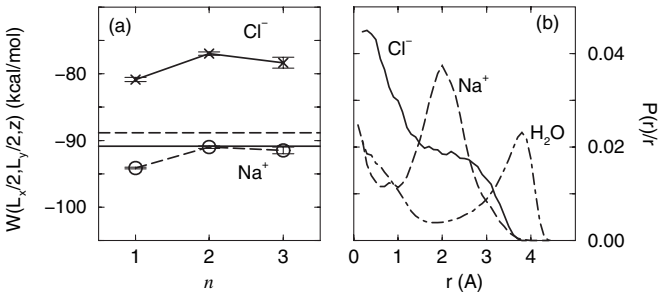

FIG. 3. (a) z-independent PMF of ions along the pore axis of a SWNT array as supercell size n varies. Solid lines/crosses: Cl^-; dashed lines/circles: Na^+. (b) Radial distribution for Cl^- (solid line), Na^+ (dashed line), and H_2O (dot-dashed line).

shell water. It may be missed by a purely dielectric continuum treatment of water [6,7,33].

In conclusion, we have shown that 11.6 Å diameter silica nanoporous membranes dramatically alter ion permeability. Hydroxylated silica pores repel (attract) Cl^- (Na^+) by $\sim$28(22) kcal/mol. Amine groups on functionalized silica pores turn into $-NH_3^+$ by abstracting protons from silanol groups. This reverses the pore polarity, and molecular force fields now predict that the pore center slightly attracts Cl^- and repels Na^+. However, Na^+ can become trapped at surface sites. Pure confinement effects are asymmetric for these ions. Based on these results, a viable way to exclude both ions may be to use alternating hydroxylated and amine-functionalized silica pore segments. In that case, ion trapping, pH and multiple ion effects, and contact ion pair formation may occur, and may strongly affect ion transport.

This work was supported by the Department of Energy under Contract No. DE-AC04-94AL85000 at Sandia National Laboratories operated by the Lockheed Martin Company for the Department of Energy.

*Corresponding author.
Email address: kleung@sandia.gov

[1] D. A. Doshi *et al.*, Science **290**, 107 (2000).
[2] N.-G. Liu, R. A. Assink, B. Smarsly, and C. J. Brinker, Chem. Commun. (Cambridge) **10**, 1146 (2003).
[3] D. Stein, M. Kruithof, and C. Dekker, Phys. Rev. Lett. **93**, 035901 (2004).
[4] R. Fan *et al.*, Phys. Rev. Lett. **95**, 086607 (2005).
[5] A. Kalra, S. Garde, and G. Hummer, Proc. Natl. Acad. Sci. U.S.A. **100**, 10 175 (2003).
[6] A. Parsegian, Nature (London) **221**, 844 (1969); P. C. Jordan, Biophys. J. **39**, 157 (1982).
[7] O. Beckstein, K.-H. Tai, and M. S. P. Sansom, J. Am. Chem. Soc. **126**, 14 694 (2004), and references therein.
[8] L. R. Pratt and S. B. Rempe, in *Simulation and Theory of Electrostatic Interactions in Solution*, edited by L. R. Pratt and G. Hummer (ALP, New York, 1999), p. 172.
[9] S. Holmann, S. Nielsen, and P. Agre, *Aquaporins* (Academic, New York, 2001).
[10] B. Roux, T. Allen, S. Berneche, and W. Im, Q. Rev. Biophys. **37**, 15 (2004).
[11] C. Dellago, M. M. Naor, and G. Hummer, Phys. Rev. Lett. **90**, 105902 (2003).
[12] A. Kohlmeyer, C. Hartnig, and E. Spohr, J. Mol. Liq. **78**, 233 (1998), and references therein.
[13] J. R. Rustad *et al.*, J. Colloid Interface Sci. **198**, 119 (1998).
[14] D. A. Litton and S. H. Garofalini, J. Appl. Phys. **89**, 6013 (2001); C. D. Lorenz *et al.*, Tribol. Lett. **19**, 93 (2005).
[15] L. T. Zhuravlev, Colloids Surf. A **173**, 1 (2000).
[16] G. Kresse and J. Furthmüller, Phys. Rev. B **54**, 11 169 (1996); Comput. Mater. Sci. **6**, 15 (1996).
[17] J. P. Perdew and Y. Wang, Phys. Rev. B **45**, 13 244 (1992).
[18] For the MD/MC codes used, see: S. J. Plimpton, J. Comput. Phys. **117**, 1 (1995); M. G. Martin and A. P. Thompson, Fluid Phase Equilib. **217**, 105 (2004).
[19] H. J. C. Berendsen, J. R. Gridera, and T. P. Straatsma, J. Phys. Chem. **91**, 6269 (1987).
[20] M. Tsige *et al.*, J. Chem. Phys. **118**, 5132 (2003).
[21] $\epsilon_{Si} = 0.1$ kcal/mol; $\epsilon_O = 0.155$ kcal/mol; $\sigma_{Si} = 4$ Å; $\sigma_O = 3.1656$ Å; $q_O = -0.60e$ ($-0.74e$) for bulk (silanol) oxygens; $q_H = 0.43e$. Each q_{Si} is adjusted to yield local charge neutrality. Optimal O-H bond length and Si-O-H angle are 0.968 Å and 120.0°, with harmonic force constants of 596 kcal/mol/Å^2 and 22.1 kcal/mol/rad^2.
[22] R. M. van Ginhoven, H. Jónsson, B.-G. Park, and L. R. Corrales, J. Phys. Chem. B **109**, 10 936 (2005).
[23] S. H. Garofalini, J. Non-Cryst. Solids **120**, 1 (1990).
[24] K. Leung and S. B. Rempe, J. Chem. Phys. **122**, 184506 (2005).
[25] A. D. MacKerell *et al.*, J. Phys. Chem. B **102**, 3586 (1998).
[26] S. Rajamani, T. Ghosh, and S. Garde, J. Chem. Phys. **120**, 4457 (2004).
[27] D. Asthagari, L. R. Pratt, and H. S. Ashbaugh, J. Chem. Phys. **119**, 2702 (2003).
[28] We use Ewald sums with tin-foil boundary conditions. We do not reference our PMF to the silica membrane surface, which can have different functionalization and charge distributions than that inside the pore. Thus our PMF excludes extrinsic potential effects [A. Redblack and J. Grindlay, J. Phys. Chem. Solids **36**, 73 (1975)]. The silica pores can be thought of as infinite cylinders with dipolar pore walls.
[29] T. Werder *et al.*, J. Phys. Chem. B **107**, 1345 (2003).
[30] C. Peter and G. Hummer, Biophys. J. **89**, 2222 (2005).
[31] Polarizable force fields predict higher Cl^- concentrations at interfaces [E. C. Brown *et al.*, J. Phys. Chem. B **109**, 7934 (2005)].
[32] P. S. Crozier *et al.*, Biophys. J. **81**, 3077 (2001). Here the pore is smaller than the Cl^- first hydration shell.
[33] M. Carrillo-Tripp, H. Saint-Martin, and I. Ortega-Blake, Phys. Rev. Lett. **93**, 168104 (2004).